Encapsulated Energy Transfer Cassettes with Extremely Well Resolved Fluorescent Outputs

Yuichiro Ueno✤, **Jiney Jose**✤, **Aurore Loudet**✤, **César Pérez-Bolívar**†, **Pavel Anzenbacher Jr.**†, and **Kevin Burgess**✤,*

†Department of Chemistry BGSU, Bowling Green, OH, 43403

✤Department of Chemistry, Texas A & M University, Box 30012, College Station, TX 77841

Abstract

This paper concerns the development of water-compatible fluorescent imaging-probes with tunable photonic properties that can be excited at a single wavelength. Bichromophoric cassettes **1a** – **1c** consisting of a BODIPY donor and a cyanine acceptor were prepared using a simple synthetic route, and their photophysical properties were investigated. Upon excitation of the BODIPY moiety at 488 nm the excitation energy is transferred through an acetylene bridge to the cyanine dye acceptor, which emits light at approximately 600, 700, and 800 nm, *ie* with remarkable dispersions. This effect is facilitated by efficient energy transfer that gives a 'quasi-Stokes' shift of between 86 – 290 nm opening a huge spectral window for imaging. The emissive properties of the cassettes depend on the energy transfer (ET) mechanism: the faster the transfer, the more efficient it is. Measurements of rates of energy transfer indicate that a through-bond energy transfer takes place in the cassettes **1a** and **1b** that is two orders of magnitude faster than the classical through-space, Förster, energy transfer (in the case of cassette **1c**, however, both mechanisms are possible, and the rate measurements do not allow us to discern between them). Thus the cassettes **1a** – **1c** are well suited for multiplexing experiments in biotechnological methods that involve a single laser-excitation source. However, for widespread application of these probes their solubility in aqueous media must be improved. Consequently, the probes were encapsulated in calcium phosphate/silicate nanoparticles (diameter *ca* 22 nm) that are freely dispersible in water. This encapsulation process resulted in only minor changes in the photophysical properties of the cassettes. The system based on cassette **1a** was chosen to probe how effectively these nanoparticles could be used to deliver the dyes into cells. Encapsulated cassette **1a** permeated Clone 9 rat liver cells where it localized in the mitochondria and fluoresced through the acceptor part, *ie* red. Overall, this paper reports readily accessible, cyanine-based through-bond energy transfer cassettes that are lypophilic but can be encapsulated to form nanoparticles that disperse freely in water. These particles can be used to enter cells and to label organelles.

Introduction

Fluorescent labels that display high photo- and chemical stability, bright fluorescence and emission wavelength tunability are important tools in cellular biology.[1,2] Such labels generally allow for high-quality images at lower photon flux, without sacrificing accuracy (low background). If the labels allow channel multiplexing then that is also an advantage as

it facilitates tracking of several components in a single experiment.[3,4] However, large Stokes' shifts are required to achieve resolutions necessary for multiplexing experiments. These shifts correspond to energies required for reorganization from ground to excited states;[5,6] for most planar, conjugated organic labels, compounds with relatively small Stokes' shifts (10–20 nm),[7] this parameter is not easily manipulated.[8,9] Thus multiplexed fluorescent labels for excitation at one wavelength must involve compromise between two opposing physical parameters.[3] If the excitation source is set at the absorption maxima of the dyes used, then all the dyes must have nearly the same absorption maxima and the limit of the resolution is defined by the Stokes' shifts of the dyes. Conversely, if the dyes are chosen for their diverse fluorescence emission maxima, then the UV absorption maxima of some of the dyes will not correspond to the excitation wavelength, these dyes will absorb less light, and they will fluoresce less brightly.

Many applications in bioimaging require probes that are compatible with aqueous media. Incorporation of water-solubilizing groups in labels is a challenge[10] and presents problems during purification[5] especially since even small amounts of fluorescent impurities may skew the data obtained in imaging experiments. Furthermore, water-solubilizing groups attached to fluors often result in decreased fluorescence intensities due to non-radiative decay processes facilitated by solvation sphere rearrangement in the excited state. [11,12] Finally, if these obstacles are overcome, the resulting labels may be highly polar; this tends to impart an increased affinity for cytoplasm making the probes less useful for imaging of other cellular compartments.

Here we present a rational design of fluorescent labels that allows tuning of fluorescent outputs through a wide emission window via cassettes composed of donor and acceptor chromophores.[8,11,13,14] Specifically, this paper describes cassettes that work via excitation of a BODIPY-based[15−18] donor with blue light (*eg* 488 nm) followed by fast energy transfer to variable cyanine-based[15,19,20] acceptors, which then emits red light. Three cassettes were prepared, **1a** – **1c** (Scheme 1). The wavelength of the emitted light depends on the structure of the acceptor, and varies from 590 to 794 nm. While the Stokes' shift of the donor is short (~ 20 nm), the red shift in the cassettes is between 86 – 290 nm; this dispersion is greater than any other achieved in cassettes generated in these laboratories.[21−29] These probes are relatively easy to make, partly because they are lipophilic, but they have poor water-solubilities. To obviate this issue, the cassettes were encapsulated in calcium phosphate/silicate nanoparticles that are freely dispersed in water. Experiments are described to elucidate how these particles can be used as delivery agents wherein the dye-containing particles become localized within the cells.

Results and Discussion

Syntheses and Spectroscopic Properties of the Cassettes

Cassettes **1a** – **1c** were prepared by cross-coupling the readily available donor fragment **D** with the iodine-functionalized cyanine dyes **2a** – **2c** (Scheme 1, and SI). These materials were easily purified via flash chromatography because they are lipophilic and colored.

Spectroscopic data for the cassettes **1** are presented in Figure 1 and Table 1. Figure 1a shows the absorbance spectra; these resemble the summation of components from the donor and acceptor fragments. When the cassettes are excited at 504 nm (the donor), **1a** and **1b** emit predominantly from their acceptor fragments; only about 10 % of the fluorescence "leaks" from the donor part. Leakage from the donor is prevalent in the fluorescent spectra of **1c** under the same conditions. Quantitatively, this parameter is reflected by the "energy transfer efficiencies" (ETEs; $\{\Phi_d/\Phi_a\} \times 100$)[29] of these cassettes (**1a** and **1b** >88 %; **1c**, 43 %).

We speculate that the difference in quantum yield for the three cassettes after encapsulation is due to the orientation of the cassettes within the particles. In case of cassette **1a** (Cy3 cassette) the fluor is well encapsulated and devoid of any π-stacking, hence its quantum yield is high. However **1b** and **1c** may be oriented in ways that favor more π-stacking, resulting in lower quantum yields.

Ultra-fast Spectroscopy Measurements

Ethynylene linkers were incorporated in cassettes **1a** – **1c** to facilitate donor-to-acceptor energy transfer through-*bonds*,[30] though through-*space* energy transfer is also plausible. Femtosecond transient spectroscopy was performed to compare actual rates of energy transfer in these systems to ones calculated for transfer through-*space* (FRET). As a control, *intermolecular* energy transfer between the donor **D** in ethanol with equimolar (3.1×10^6 M) concentration of non-iodinated analog of the acceptors (**2a**, Cy3) was also studied. Energy transfer did occur under these conditions, at a rate of 1.85×10^9 s^{-1}.

Energy transfer rates were measured for the cassettes **1a** – **1c** (at the concentration of 3.1×10^{-6} M) and compared with the rates calculated for through-*space* energy transfer using the Förster model (Table 2). From the perspective of the resonance energy transfer (RET) theory, the overlap integral J for the emission of the donor (common for the three cassettes) and the absorption of the indocyanine acceptor (Figure 2) show a step-wise decrease **1a** > **1b** > **1c** while the Förster radius (R_0) increases. Following the Förster model, the calculated theoretical value for the resonance energy transfer decreases from 8.59×10^9 for **1a** to 1.88×10^9 (**1b**), and 1.39×10^9 (**1c**), respectively (Table 2). Consequently, the Förster energy transfer rate calculated for cassette **1a**, for instance, was approximately four times faster than the observed rate for the intermolecular transfer in the control described above.

Observed energy transfer rates for cassettes **1a** – **1b** were two orders of a magnitude higher than the rates predicted for the Förster model. Specifically, the rates for **1a** and **1b** are 56 and 67 times faster than the ones calculated for through-space energy transfer (Table 2). These data suggest a dramatic effect of the donor-acceptor communication through the phenylethyne bridge.

Cassette **1c** shows an energy transfer rate equal (within 10% error) to the through-*space* energy transfer rate following the Förster model. This suggests that in **1c** the resonance energy transfer proceeds through-*space* or in a mixed through-*space* and through-*bond* mechanism. Overall, the measured rates suggest the efficiency decreases from 90 to 87 and 43% for **1a**, **1b** and **1c**, respectively.

On a picosecond-timescale, energy transfer was observed by following the concerted kinetics of the donor stimulated emission decay following the excitation and the population of the acceptor excited state following the bleaching of the donor. After the energy is transferred, the acceptor decays at its usual timescale, *ie* as if excited directly. For example, excitation of cassette **1a** at the donor (420 nm) by a femtosecond laser pulse is followed by the decay of a singlet state, which is complete within 2.1 ps and is accompanied by the population of an acceptor excited state with 2.2 ps raise time. Thereafter, the acceptor decays with a fluorescence lifetime of 352 ps by emitting with a λ_{max} of 600 nm (Figure 3). Similarly, exciting cassette **1b** at 420 nm results in singlet state population of the BODIPY donor, decay within 8.0 ps, then complete population of the acceptor excited state after 9.6 ps; the acceptor singlet excited state decays with a fluorescence lifetime of 840 ps (λ_{max} = 680 nm). In contrast to the other two cassettes, the donor of **1c** decays slowly (within 800 ps) which suggests that the excited state of the donor is not being depopulated by a strongly coupled acceptor as it is in the cassettes **1a** and **1b**, and the energy transfer is less efficient.

Through-*space* RET is still operational in the cassette **1c** since the donor alone decays with a lifetime of 4 ns which is comparable to the 800 ps rate in the cassette.

The following conclusions can be drawn from the measurement of energy transfer rates. First, a significantly more efficient pathway for donor-acceptor communication exists for cassettes **1a** and **1b** than compared to that in **1c**. Aryl-ethynyl-aryl moieties display a strong electronic coupling[30] and this suggests that the energy transfer takes place through the bridge. The efficiency and rate of the energy transfer processes in **1a** and **1b** are a strong indication of an exciton hopping mechanism.[31–34] Cassette **1c** transfers energy at a rate that can be rationalized using the Förster through-*space* model.

Encapsulation of the Dyes In Calcium Phosphate/silicate

Cassettes **1a** – **1c** are not water-soluble, but we show here they can be encapsulated in calcium phosphate to form nanoparticles. With respect to biotechnological applications, calcium phosphate is an excellent matrix for nanoparticle encapsulation because: (i) moderate concentrations of Ca^{2+} ions are not toxic to cells; (ii) it is not toxic *in vivo* (found in human bone, and teeth); (iii) it is claimed that calcium phosphate dissolves below pH 5.5 to liberate the cargo, but is stable at 7.4;[35] (iv) particles of this matrix disperse freely in aqueous media; and, (v) the surface of these particles can be functionalized.[36,37] Adair and co-workers have shown that spherical, *ca* 18 nm diameter, calcium phosphate nanoparticles can be formed with citrate-derived surface carboxylate groups and fluorescent dye cargoes.[38] They have investigated these particles for imaging, in cells and *in vivo*.[39–43]

In our work, calcium phosphate nanoparticles encapsulating cassettes **1a** – **1c** were prepared via Adair's procedure[38] except that a longer reaction time was used (24 h, not 5 min), the particles were purified via MPLC rather than HPLC, and finally a dialysis step was performed to transfer the particles from an ethanolic to an aqueous media. Figure 4 shows AFM images of the particles formed from the cassettes **1**; these are quite uniform with diameters around 22 nm.

Spectroscopically, encapsulated cassettes **1a** – **1c** had absorption and fluorescent spectra that are almost identical to those of the free cassettes in EtOH (see Table 1). The quantum yield of encapsulated **1a** –**CaNP** increased about 30 % relative to the free dye in EtOH, but for **1b-CaNP** and **1c-CaNP** it decreased by 5- and 2-fold respectively, but is satisfactory for some applications. Throughout, the energy transfer efficiencies were essentially unchanged.

Permeation of The Particles Into Clone 9 Rat Liver Cells

Cassette **1a** and **1a-CaNPs** were imported in Clone 9 cells at 37 °C to study their subcellular localization. Cassette **1a** was observed in different organelles: the mitochondria, the lysosomes, the ER and the cytoplasm. Interestingly, the emission output observed was dependent on the subcellular compartment. Thus, in the mitochondria, perfect energy transfer was observed *ie* only emission from the cyanine was seen hence the probes fluoresced red. Diffuse *green* fluorescence was observed in the cytoplasm and ER, and in some bright punctates (lysosomes); the green fluorescence is indicative of emission from the donor part. Conversely, **1a-CaNPs** localized only in the mitochondria, and sole emission from the cyanine part was observed, *ie* the dyes fluoresced red (Figure 5). When the cells were treated with **1a-CaNPs** at 4 °C, no fluorescent signal could be observed after 2 h incubation, indicating that the nanoparticles may enter via endocytosis.

Conclusions

The research described here represents the first report of coupling BODIPY-based donors with *cyanine* acceptors in ways that facilitate energy transfer through-*bonds*. The dispersion

of fluorescence emissions from these cassettes is greater than any others prepared by us or, to the best of our knowledge, by others. The observed energy transfer rates for cassettes **1a** and **1b** are significantly faster than for dipole-dipole coupling in a through-*space* manner, indicating transfer through bonds is indeed occurring. Overall, they are excellent tools for fluorescence multiplexing in biotechnology.

Syntheses of such cassettes are straight-forward because they are lipophilic. The idea of using water-dispersible nanoparticles to bring lipophilic *cassettes* into aqueous media, thereby circumventing syntheses of water-soluble materials, is novel, and has the potential to be applied to other donor-acceptor systems where water-soluble modifications would be hard to make. The absorbance and emission maxima of the *cassettes* and the extent of donor-acceptor energy transfer (E.T.E) remained significantly unchanged after encapsulation into nanoparticles. Conversely, and surprisingly, the fluorescence quantum yields of the three systems studied in this paper were significantly effected. Thus, the fluorescence quantum yield for **1a-CaNPs** increased by about 30% relative to the free dye in EtOH, while for **1b-CaNPs** and **1c-CaNPs** it decreased by 5- and 2-fold respectively. Nanoparticles encapsulating these cassettes may have applications for intracellular imaging, and for observation of parallel macroscopic events *in vivo*, *eg* as labels for targeting different cancer forms simultaneously, and allowed specific targeting of organelles. Other applications beyond organelle targeting in cells can now be envisaged.

Supplementary Material

Refer to Web version on PubMed Central for supplementary material.

Acknowledgments

References

1. Sauer, M.; Hofkens, J.; Enderlein, J. Handbook of Fluorescence Spectroscopy and Imaging: From Ensemble to Single Molecules. Weinheim: Wiley-VCH; 2010.

2. Sabnis, RW. Handbook of Biological Dyes and Stains. Synthesis and Industrial Applications. Hoboken: Wiley & Sons; 2010.

3. Levenson RM, Mansfield JR. Cytometry. 2006; 69:748–758. [PubMed: 16969820]

4. Haney, SA. High Content Screening: Science, Techniques and Applications. Hoboken: Wiley-Interscience; 2008.

5. Delmotte C, Delmas A. Bioorg. Med. Chem. Lett. 1999; 9:2989–2994. [PubMed: 10571161]

6. Taylor, DL.; Haskins, JR.; Giuliano, KA. High Content Screening: A Powerful Approach to Systems Cell Biology and Drug Discovery. Vol. Vol. 356. Totowa, NJ: Humana Press; 2007.

7. Montalti, M.; Credi, A.; Prodi, L.; Gandolfi, MT. Handbook of Photochemistry. 3rd ed.. Boca Raton, FL: CRC Press-Taylor & Francis; 2006.

8. Wang L, Tan W. Nano Lett. 2006; 6:84–88. [PubMed: 16402792]

9. Lakowicz, JR. Principles of Fluorescence Spectroscopy. 3rd ed.. New York: Springer; 2006.

10. Romieu A, Brossard D, Hamon M, Outaabout H, Portal C, Renard P-Y. Bioconjugate Chem. 2008; 19:279–289.

11. Forster T. Naturwissenschaften. 1946; 6:166–175.

12. Laia CAT, Costa SMB. Chemical Physics Letters. 1998; 285:385–390.

13. Zhu L, Soper SA. Rev. Fluoresc. 2006; 3:525–574.

14. Lakowicz, JR. Principles of Fluorescence Spectroscopy. Second ed.. New York: Kluwer Academic/Plenum Publishers; 1999.

15. Loudet, A.; Burgess, K. Handbook of Porphyrin Science: With Applications to Chemistry, Physics, Materials Science, Engineering, Biology and Medicine. Kadish, K.; Smith, K.; Guilard, R., editors. World Scientific; 2010. p. 203

16. Ulrich G, Ziessel R, Harriman A. Angew. Chem. Int. Ed. 2008; 47:1184–1201.

17. Ziessel R, Ulrich G, Harriman A. New J. Chem. 2007; 31:496–501.

18. Loudet A, Burgess K. Chem. Rev. 2007; 107:4891–4832. [PubMed: 17924696]

19. Mishra A, Behera RK, Behera PK, Mishra BK, Behera GB. Chem. Rev. 2000; 100:1973–2011. [PubMed: 11749281]

20. Ozhalici-Unal H, Pow CL, Marks SA, Jesper LD, Silva GL, Shank NI, Jones EW, Burnette JM III, Berget PB, Armitage BA. J. Am. Chem. Soc. 2008; 130:12620–12621. [PubMed: 18761447]

21. Burgess, K.; Burghart, A.; Chen, J.; Wan, C-W. Proc. SPIE-Int. Soc. Opt. Eng. Vol. Vol. 3926. San Jose, CA: 2000. p. 95-105.

22. Burghart A, Thoresen LH, Chen J, Burgess K, Bergstrom F, Johansson LB-A. Chem. Commun. 2000:2203–2204.

23. Jiao G-S, Thoresen Lars H, Burgess K. J. Am. Chem. Soc. 2003; 125:14668–14669. [PubMed: 14640617]

24. Wan C-W, Burghart A, Chen J, Bergstroem F, Johansson LBA, Wolford MF, Kim TG, Topp MR, Hochstrasser RM, Burgess K. Chem.--Eur. J. 2003; 9:4430–4441.

25. Burgess, K. US Patent No. US2005/0032120 A1 U.S. Patent 2005/0032120 A1. 2005. p. 7

26. Bandichhor R, Petrescu AD, Vespa A, Kier AB, Schroeder F, Burgess K. J. Am. Chem. Soc. 2006; 128:10688–10689. [PubMed: 16910657]

27. Kim TG, Castro JC, Loudet A, Jiao JGS, Hochstrasser RM, Burgess K, Topp MR. J. Phys. Chem. A. 2006; 110:20–27. [PubMed: 16392835]

28. Jose J, Ueno Y, Wu L, Loudet A, Chen H-Y, Son DH, Burgess K. Chem. Commun. 2009 submitted.

29. Wu L, Loudet A, Barhoumi R, Burghardt RC, Burgess K. J. Am. Chem. Soc. 2009; 131:9156–9157. [PubMed: 19566090]

30. Polyansky DE, Danilov EO, Voskresensky SV, Rodgers MAJ, Neckers DC. J. Am. Chem. Soc. 2005; 127:13452–13453. [PubMed: 16190681]

31. Davis WB, Svec WA, Ratner MA, Wasielewski MR. Nature. 1998; 396:60–63.

32. Kim D, Osuka A. Acc. Chem. Res. 2004; 37:735–745. [PubMed: 15491120]

33. Montes VA, Perez-Bolivar C, Estrada LA, Shinar J, Anzenbacher P Jr. J. Am. Chem. Soc. 2007; 129:12598–12599. [PubMed: 17902661]

34. Montes VA, Perez-Bolivar C, Agarwal N, Shinar J, Anzenbacher P Jr. J. Am. Chem. Soc. 2006; 128:12436–12438. [PubMed: 16984192]

35. Bisht S, Bhakta G, Mitra S, Maitra A. Int. J. Pharm. 2005; 288:157–168. [PubMed: 15607268]

36. Altinoglu EI, Russin TJ, Kaiser JM, Barth BM, Eklund PC, Kester M, Adair JH. ACS Nano. 2008; 2:2075–2084. [PubMed: 19206454]

37. Morgan TT, Muddana HS, Altinoglu EI, Rouse SM, Tabakovic A, Tabouillot T, Russin TJ, Shanmugavelandy SS, Butler PJ, Eklund PC, Yun JK, Kester M, Adair JH. Nano Lett. 2008; 8:4108–4115. [PubMed: 19367837]

38. Altinoglu EI, Russin TJ, Kaiser JM, Barth BM, Eklund PC, Kester M, Adair† JH. ACS Nano. 2008:2075–2086. [PubMed: 19206454]

39. Morgan TT, Muddana HS, lu EIA, Rouse SM, Tabakovic A, Tabouillot T, Russin TJ, Shanmugavelandy SS, Butler PJ, Eklund PC, Yun JK, Kester M, Adair JH. Nano Lett. 2008; 8:4108–4115. [PubMed: 19367837]

40. Muddana HS, Morgan TT, Adair JH, Butler PJ. Nano Lett. 2009:1559–1566. [PubMed: 19260707]

41. Kester M, Heakal Y, Fox T, Sharma A, Robertson GP, Morgan TT, Altinoglu EI, Tabakovic A, Parette MR, Rouse S, Ruiz-Velasco V, Adair JH. Nano Lett. 2008; 8:4116–4121. [PubMed: 19367878]

42. Gupta R, Mishra P, Mittal A. J. Nanosci. Nanotechnol. 2009; 9:2607–2615. [PubMed: 19438010]

43. Glowka E, Lamprecht A, Ubrich N, Maincent P, Lulek J, Coulon J, Leroy P. Nanotechnology. 2006; 17:2546–2552. [PubMed: 21727503]
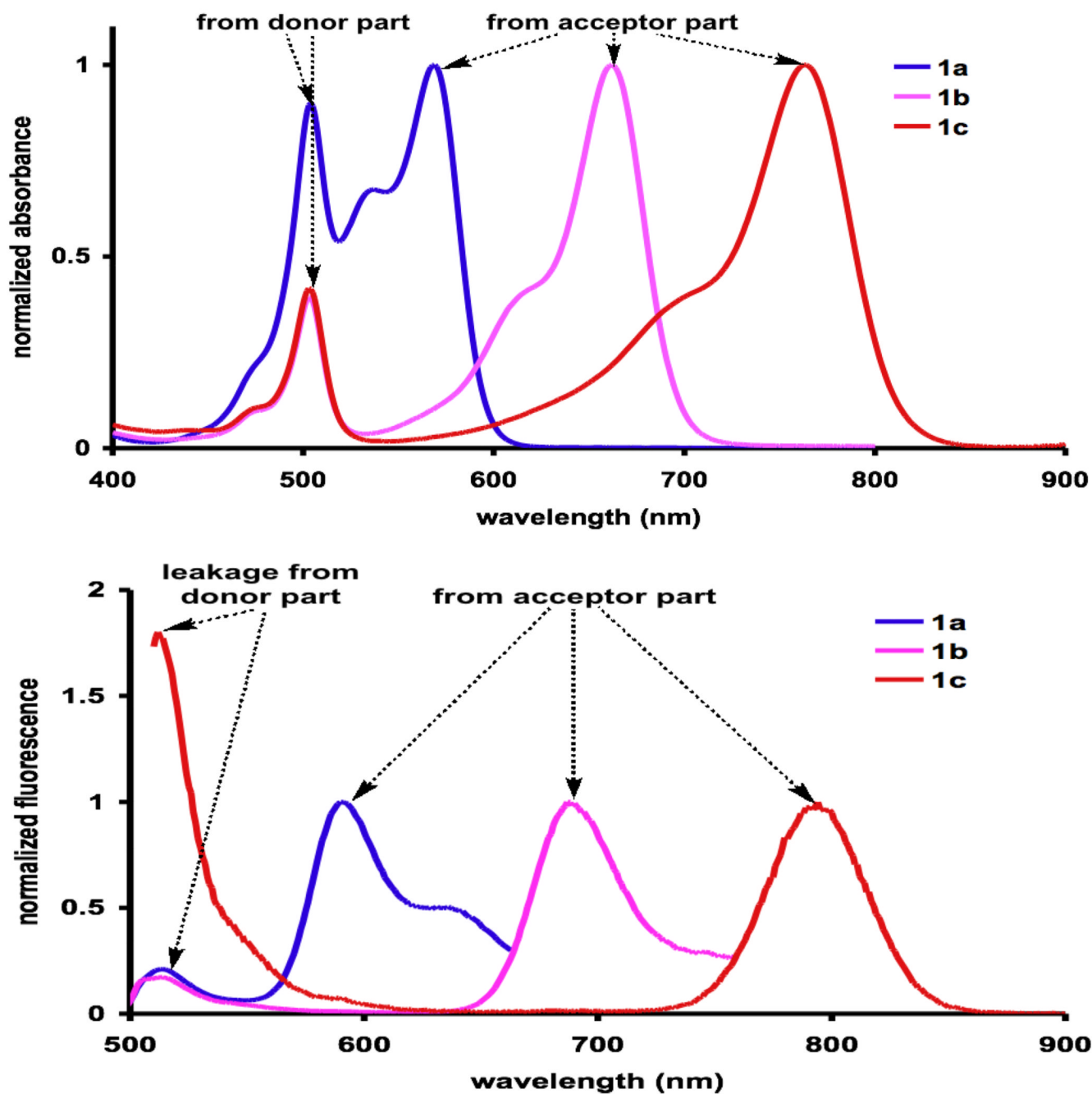
Figure 1.
Normalized **a** absorbance and **b** fluorescence spectra of the cassettes in EtOH (at 10^{-6} and 10^{-7} M for absorbance and fluorescence measurements, respectively).
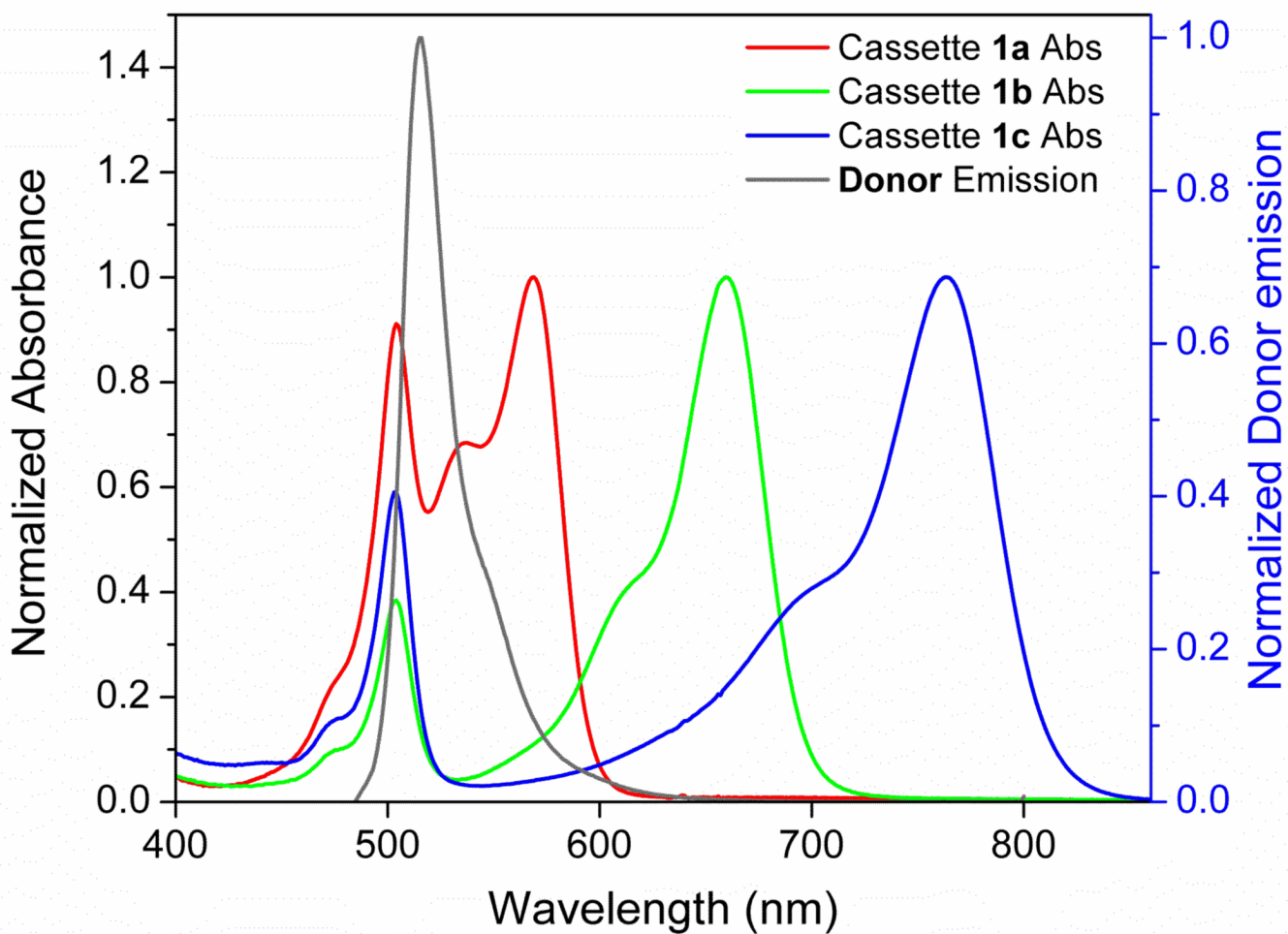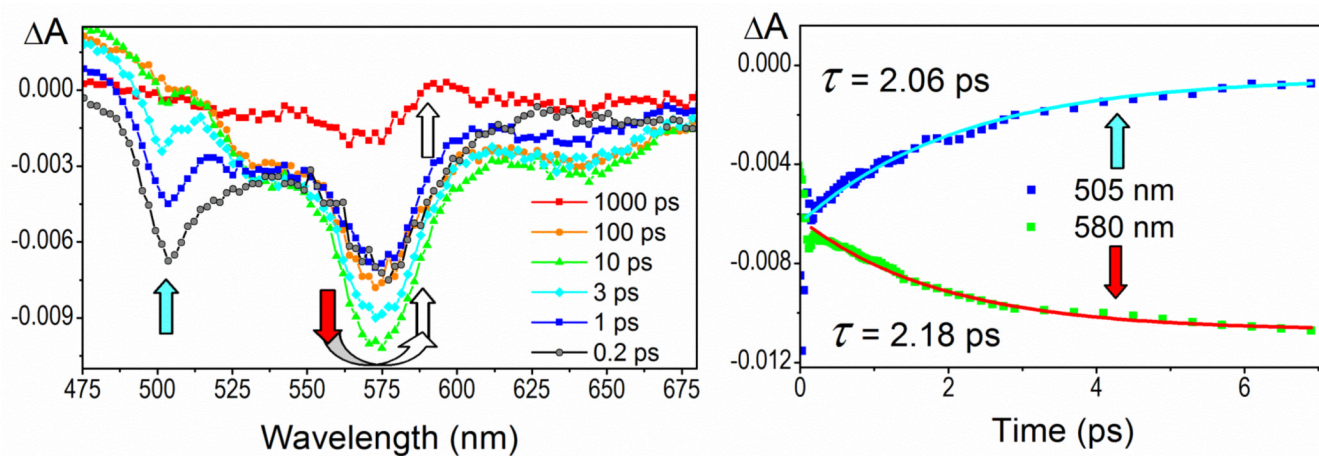
Figure 2.
Spectral overlap of BODIPY donor emission (▬) and cassette absorption (**1a** ▬; **1b** ▬; **1c** ▬) ensures resonance energy transfer (RET).

Figure 3.
Left: Transient absorption spectra of the cassette **1a** showing a concerted depletion of the stimulated emission donor maximum at 505 nm (blue arrow) and raise of the acceptor maxima at 580 nm (red arrow) followed by acceptor relaxation within 350 ps. Right: Kinetic profiles of the donor decay (2.06 ps) and acceptor raise (2.18 ps) reflect the concerted process.
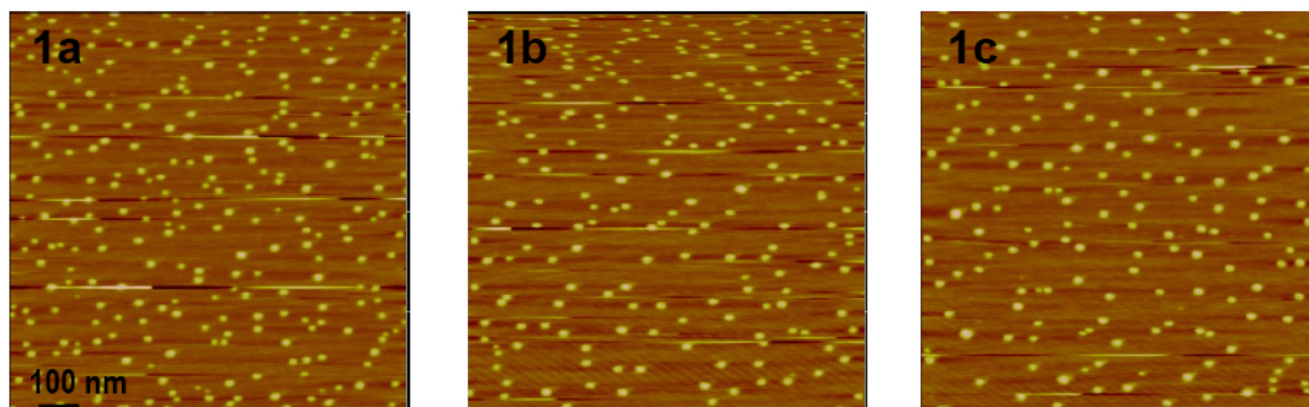
Figure 4.
Atomic force microscopy (AFM) images of cassettes encapsulated calcium phosphate
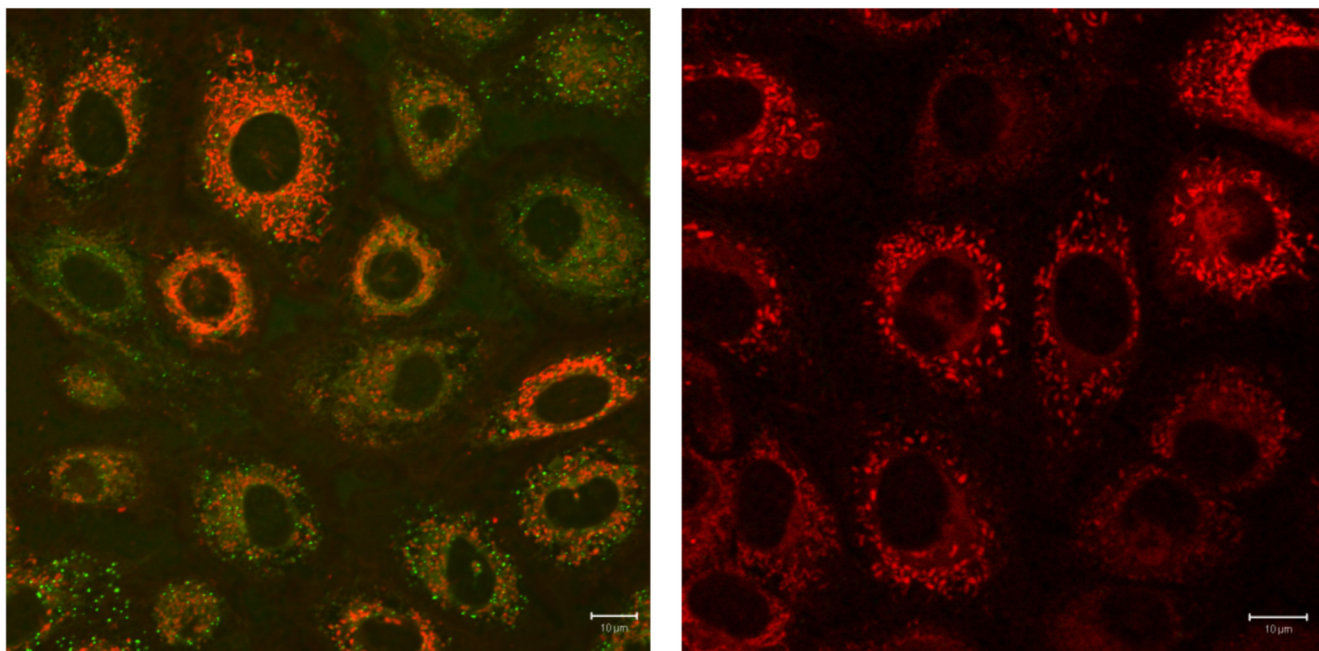nanoparticles. Avg. particle size: 22 nm.

Figure 5.
Fluorescence images of cassette **1a** (*left*) and **1a-CaNP** (*right*) in normal rat liver cells (Clone 9). Scale bar is 10 µm.

donor

acceptors

n = 0; **2a**, 1; **2b**, 2; **2c**

$Pd(PPh_3)_4$, CuI, Et_3N
DMF, 40 °C, 1 h

twisted π-conjugated inker

504 nm

a; 590, **b**; 687
c; 794 nm

n = 0; **a** 45 %, 1; **b** 26 %, 2; **c** 33 %

1
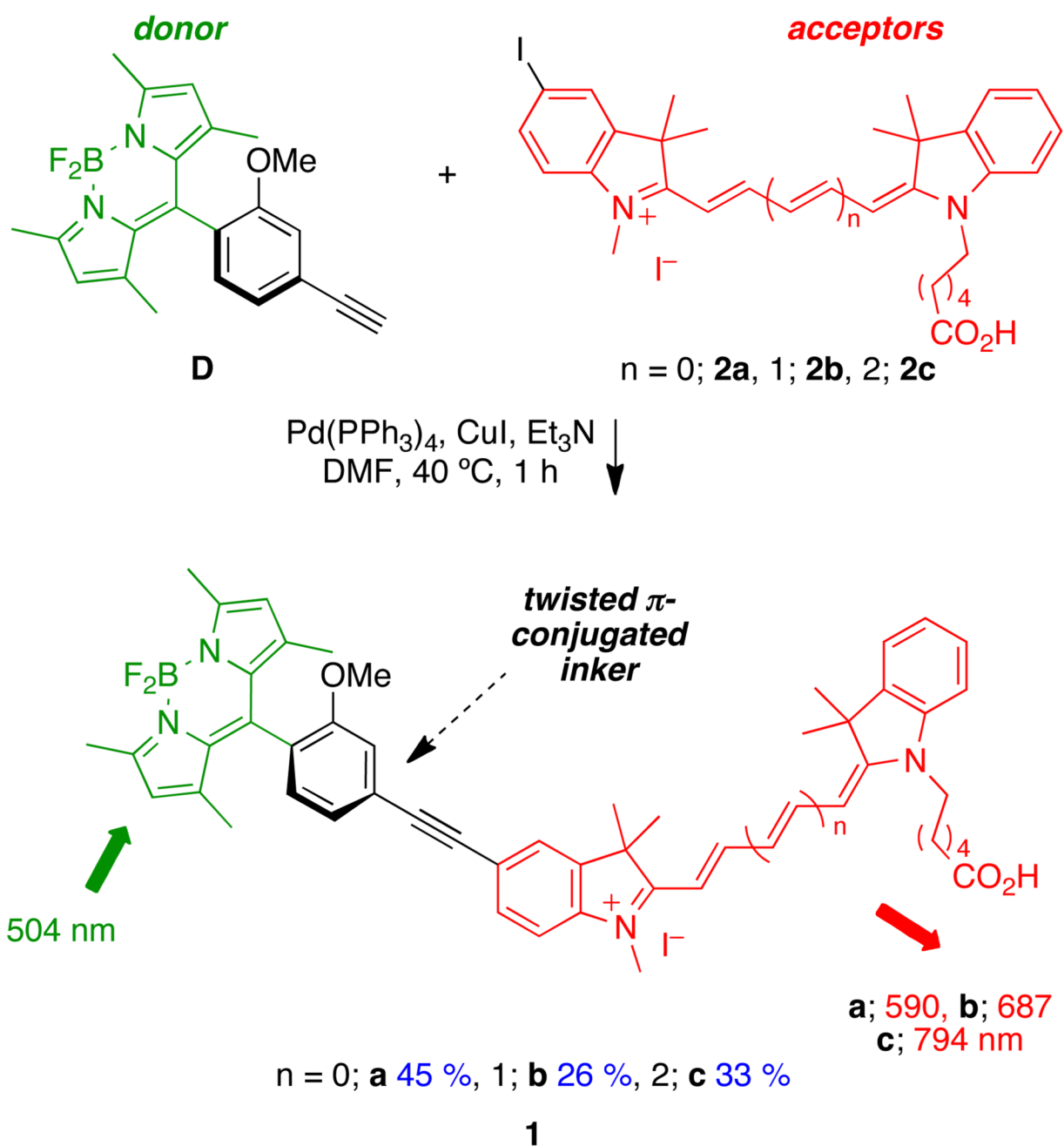
Scheme 1.
Syntheses of the TBET-cassettes **1a**, **1b**, **1c**.

Table 1

Photophysical properties of cassettes

	λ_{abs}	λ_{emiss}	$\Phi_d{}^a$	$\Phi_a{}^b$	ETE (%)
in EtOH					
1a	504, 569	519, 590	0.20+/−0.01	0.22+/−0.02	90
1b	504, 662	519, 687	0.35+/−0.02	0.40+/−0.03	87
1c	504, 763	519, 794	0.11	_^{c}	43^d
nanoparticles in pH 7.4 phosphate buffer					
1a	504, 568	519, 592	0.26+/−0.01	0.29+/−0.02	88
1b	504, 659	519, 687	0.063	0.071	89
1c	504, 764	519, 793	0.053	_^{c}	41^d

$^a\Phi_d$: Φ of acceptor when excited at donor relative to rhodamine 6G (Φ 0.92 in EtOH);

$^b\Phi_a$: Φ of acceptor when excited at acceptor relative to rhodamine 101 for **1a** (Φ 1.0 in EtOH), and Nile Blue for **1b** (Φ 0.27 in EtOH). Quantum yields were measured three times and averaged, and were corroborated using the absolute fluorescence quantum yield measurements. ETE: energy transfer efficiency (Φ_d/Φ_a) × 100.

^{c}No appropriate standard due to range of wavelengths.

^{d}See SI for calculation.

Table 2

Energy transfer data calculated and recorded using time-resolved fluorescence spectroscopy and femtosecond transient spectroscopy in ethanol at 22 °C.

Cassette	Transfer rate measured (s^{-1})	Förster radius calcd. R_0 (Å)	Overlap int. J (M^{-1} cm^3 nm^4)	Transfer rate calcd. (s^{-1}) [a]	Measured ET efficiency (%)	Donor decay (ps)	Acceptor raise (ps)	Acceptor decay (ps)
1a	4.85×10^{11}	129	3.47×10^{17}	8.59×10^9	90	2.06	2.18	352
1b	1.26×10^{11}	100	7.61×10^{16}	1.88×10^9	87	7.96	9.55	~1000
1c	1.26×10^9	94	5.14×10^{16}	1.39×10^9	43	794	ND [b]	719

[a] Transfer rate for the Förster through-*space* ET was calculated using r (donor-acceptor distance) determined as an average center-to-center distance using $k_T(r) = R_0^6/\tau_D$, $\chi^2 = 2/3$. r^6 formula and $r = 66.41$ Å.

[b] Relatively fast population of the acceptor singlet excited state occurred due to the direct pumping of the acceptor absorption by the laser (**1c**: $\varepsilon_{420} = 9800$ M^{-1}cm^{-1}).